PHYSICAL REVIEW E VOLUME 50, NUMBER 2 AUGUST 1994

Extraction of the bridge function for simple liquids from a molecular dynamics simulation and its application for correcting the pair distribution function

Shaw Kambayashi
Computing and Information Systems Center, Japan Atomic Energy Research Institute,
Tokai, Naka, Ibaraki 319-11, Japan

Junzo Chihara
Solid State Physics Laboratory, Japan Atomic Energy Research Institute,
Tokai, Naka, Ibaraki 319-11, Japan

(Received 17 March 1994)

Isokinetic molecular dynamics (MD) simulations have been performed for 4000 and 32 000 particles interacting via a model potential that is appropriate to liquid aluminum and the Lennard-Jones potential. Using the hypernetted-chain approximation to extrapolate the pair distribution function (PDF) obtained by the MD simulations, the bridge function is extracted for different cutoff radii of the pair potential and system sizes. We find that the extracted bridge function is almost independent of the cutoff radius used in the MD simulation. Furthermore, the bridge function is efficiently obtained by taking the extrapolating distance to be short, about 3 to 4 interatomic spacings, even in the case of the small-size simulation, with a discarding of the PDF data outside that distance. By solving the integral equation coupled with the correctly extracted bridge function, the PDF for the pair potential without any truncation is calculated for liquid aluminum whose effective ion-ion potential is accompanied by a long-ranged Friedel oscillation. It is found that this integral equation successfully corrects the error, if any exists, in the MD PDF caused by the truncation of the pair potential, resulting in good agreement with that from a large-size simulation for a sufficiently large cutoff radius. Thus we have shown a method for obtaining the PDF for the full potential from the small-size simulation with a short cutoff potential, on the basis of the fact that the bridge function is insensitive to the truncation of the potential. At the same time, this method gives an alternative procedure to extend the MD PDF to the whole range of distances.

PACS number(s): 61.20.Gy, 61.20.Ja, 61.25.Mv

I. INTRODUCTION

In principle, if the bridge function $B(r)$ is given beforehand, the pair distribution function (PDF) of a liquid with spherically symmetric pair potential $u(r)$ is determined from the solution of the integral equation for liquids [1]: the Ornstein-Zernike relation

$$h(r) - c(r) = \rho \int h(r')c(|\mathbf{r} - \mathbf{r}'|)d\mathbf{r}' = \gamma(r) \qquad (1)$$

coupled with the closure relation

$$g(r) = h(r) + 1 = \exp[-\beta u(r) + \gamma(r) + B(r)]\,. \qquad (2)$$

Here $c(r)$ is the direct correlation function, ρ the number density, and β the inverse temperature $(k_B T)^{-1}$. Practically, the detailed knowledge of the bridge function is necessary in calculations of the PDF using the integral equation for a given potential and thermodynamic parameters. Even though $B(r)$ can be expanded in terms of h-bond elementary diagrams [1], the convergence of this expansion is too slow to be applicable to practical calculations for dense liquid state. Because of such a difficulty in the calculation of $B(r)$, various approximations have been proposed to obtain a self-consistent solution of the integral equation. For example, the hypernetted-chain (HNC) and Percus-Yevick (PY) approximations are equivalent to substituting in Eq. (2) $B(r) = 0$ and $-\gamma(r) + \ln[1 + \gamma(r)]$, respectively [1].

The reliability of an approximate integral equation can be tested by comparing its solution with the result obtained by computer simulations. During past decade, based on a universality of the bridge function pointed out by Rosenfeld and Ashcroft [2], several approximate bridge functions [2–4] for hard-sphere fluids have been proposed in the parametrized form to be used in Eq. (2) and found to yield a better description up to the freezing point than the HNC or the PY approximation. These approximations essentially share the same class of the short-range part of the bridge function which is responsible for thermodynamic quantities such as the internal energy and equation of state. However, it has been questioned that these parametrized hard-sphere bridge functions can be used as a universal function of $B(r)$ for an entire range of distances because (i) it is not clear whether the intermediate-range part of the bridge function holds a universality for various classes of simple liquids [5]; (ii) there are several approaches in calculating an approximate bridge function for hard-sphere fluids, resulting in different behavior of the intermediate-range part of the bridge function [6–8]; and (iii) these approximate integral equations do not always reproduce a correct behavior of the PDF at intermediate distances [9] even though

1063-651X/94/50(2)/1317(8)/$06.00

a specific choice of the bridge function can be adopted for particular systems [10].

Essentially, the bridge function can be calculated if complete data for $g(r)$ are available with the use of Eqs. (1) and (2). Although the computer simulation provides a PDF without any approximation to the many-body problem, the information is limited only within the half of the side length of the simulation cell. This causes a difficulty in calculating the bridge function from results of computer simulations due to unavoidable truncation error in the Fourier transform of $h(r)$. Furthermore, the computer simulation may yield different PDF's depending on the cutoff radius of the potential used in the simulation especially for liquid metals whose effective ion-ion potential is accompanied by a long-ranged oscillatory tail [11]. Hence it is necessary to see the dependence of the bridge function on the cutoff radius for its reasonable comparison with theoretically predicted $B(r)$.

The aim of this paper is to investigate the bridge function at intermediate and large distances on the basis of results of the molecular dynamics (MD) simulations of up to 32 000 particles for the Lennard-Jones (LJ) fluid and liquid aluminum and to find a method for obtaining the correct PDF in the whole distances from a small-size simulation with a truncated potential. In Sec. II we give a brief description of the models considered and our MD simulation procedure. We then present an extrapolating procedure [12–15] for raw PDF data of computer simulations with the HNC approximation [16] and the extracted bridge function together with results of approximate theories in Sec. III. It is found that the extracted bridge function depends less on the cutoff radius used in the MD simulation and that the bridge function can be efficiently obtained by taking the extrapolating distance to be as short as 3 or 4 interatomic spacings even in the small-size simulation. The short-range part of the extracted bridge function agrees well with parametrized hard-sphere bridge functions, but its intermediate-range part cannot be reproduced by that for hard-sphere fluids due to a significant dependency of the bridge function on the pair potential. Section IV is devoted to the application of the extracted bridge function for correcting the raw PDF data by substituting the extracted bridge function into Eq. (2). We find that the integral equation (2) with the extracted bridge function successfully improves the cutoff error in the raw PDF for liquid aluminum, resulting in good agreement with the simulation data for a sufficiently large cutoff radius. On the other hand, for the LJ fluid, this integral equation provides completely the same result as the raw PDF data, but gives a precise procedure for extending the MD PDF to the entire range of distances.

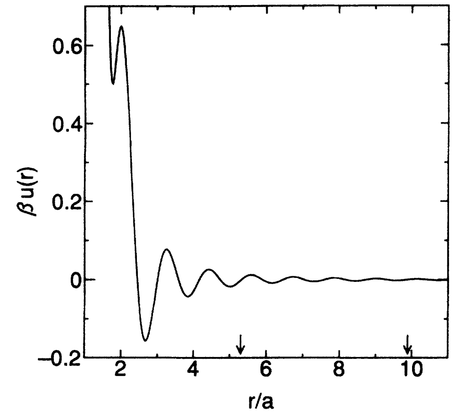

FIG. 1. Effective ion-ion potential for liquid aluminum at $T = 943$ K and mass density of 2374.35 kg m^{-3} ($r_s = 2.164$ in units of the Bohr radius a_B). The simulation is performed for two kind of cutoff potentials at $R_c = 5.31a$ and $9.89a$ indicated by the arrows.

II. MODELS AND MOLECULAR DYNAMICS SIMULATION

A. Models

We consider two different model liquids to investigate the bridge function: the LJ fluid characterized by the potential

$$u(r) = 4\varepsilon\left[\left(\frac{\sigma}{r}\right)^{12} - \left(\frac{\sigma}{r}\right)^{6}\right] \qquad (3)$$

and liquid aluminum with a model potential as described below. The model potential for aluminum is constructed by the use of the empty-core pseudopotential [17] for $\hat{u}_{ps}(q)$ in the usual expression of the effective potential for a liquid metal ($Z = 3$)

$$\hat{u}(q) = \frac{4\pi Z^2 e^2}{q^2} + \frac{q^2}{4\pi e^2}\left(\frac{1}{\epsilon(q)} - 1\right)|\hat{u}_{ps}(q)|^2 , \qquad (4)$$

with

$$\epsilon(q) = 1 - \frac{4\pi e^2}{q^2}\chi(q)\left(1 + \frac{4\pi e^2}{q^2}G(q)\chi(q)\right)^{-1} . \qquad (5)$$

Here $\chi(q)$ is the Lindhard susceptibility function and $G(q)$ is the local field correction; we have taken a simpler expression for $G(q)$ introduced by Taylor [18], which is almost equivalent numerically to that of Geldart and Taylor [19]. The parameter r_c in the empty-core pseudopotential is chosen to be $r_c = 1.12a_B$ [20], which is frequently used as a standard value for aluminum. The effective ion-ion potential for liquid aluminum is calculated in tabular form on a grid with a mesh size of 0.025 in units of the ion-sphere radius a. As seen from Fig. 1, the effective ion-ion potential for liquid aluminum shows the well known long-ranged Friedel oscillation which represents a characteristic difference to the LJ potential. As we will see in Sec. IV, this causes a different structure depending on the cutoff radius.

B. Simulation

By applying the cubic periodic boundary conditions, MD simulations have been performed for 4000 particles over 100 000 time steps and 32 000 particles over 50 000 time steps for each model liquids at the thermodynamic state near the melting point: $k_BT/\varepsilon = 0.719$

and $\rho\sigma^3 = 0.85$ for the LJ fluid, and $T = 943$ K with mass density of 2374.35 kg m^{-3} (the electron-sphere radius $r_s = 2.164$ in units of the Bohr radius a_B) for liquid aluminum. The pair potential is truncated to be used in the simulations at cutoff radius R_c: $R_c = 4.2\sigma$ for LJ fluid and for liquid aluminum two different cutoff radii $R_c = 5.31a$ and $9.89a$ in order to test effects of the long-range Friedel oscillation. For liquid aluminum, R_c is located at the node of the Friedel oscillation. These cutoff radii correspond to about 10–20 % of the side length of the simulation cell, $L = 51.18a$, for the system with the particle number $N = 32\,000$.

In our simulations, the number density is kept constant and the temperature is scaled to achieve the desired value. Throughout the present work, an isokinetic constraint by Hoover *et al.* has been applied to the equations of motion in order to maintain the temperature [21]. The equations of motion are integrated by a fifth order differential algorithm [22] with the time increment $\Delta t = 0.0025\rho^{-1/3}(m\beta)^{1/2}$, which corresponds to 6.582 fs for the LJ fluid with potential parameters for liquid argon and 1.235 fs for liquid aluminum, respectively. The integration error was monitored by examining the following consistency measure Δ [21,23]:

$$\Delta = \int_0^t \zeta(s)ds - \frac{\beta}{3N}[U(0) - U(t)] , \qquad (6)$$

with the isokinetic parameter ζ defined by

$$\zeta = \frac{\beta}{3N}\sum_{i=1}^{N} \dot{\mathbf{r}}_i(t) \cdot \mathbf{F}_i(t) . \qquad (7)$$

Here $U(t)$ is the configurational internal energy of the system at time t, ζ is the isokinetic control parameter, $\mathbf{r}_i(t)$ is the position of particle i at time t, and $\mathbf{F}_i(t)$ is the force acting on particle i at time t. For whole simulations, Δ was achieved to be less than 0.003 % relative to the internal energy per particle.

All simulations have been carried out on a vector-parallel processor Monte-4 computer [24] at Computing and Information Systems Center of Japan Atomic Energy Research Institute. The computational time required for 10 000 time steps is about 32 h for $N = 32\,000$ including the sampling of the PDF.

III. EXTRACTION OF THE BRIDGE FUNCTION

A. Numerical procedure and results

In order to extract the bridge function from the PDF calculated by MD simulation, we have applied an extrapolation technique of the PDF for $r \geq L/2$ based on that proposed by Verlet [12]. Verlet's extrapolation scheme assumes a hypothetical closure relation which includes numerical data of the PDF obtained from the MD simulation as follows:

$$g(r) = \begin{cases} g_{\mathrm{MD}}(r) , & r < R \quad (8a) \\ \exp[-\beta u(r)][1 + \gamma(r)] , & r \geq R . \quad (8b) \end{cases}$$

Here $g_{\mathrm{MD}}(r)$ is the PDF obtained from the MD simulation and $R \leq L/2$ the extrapolating distance. The right-hand side of Eq. (8b) is equivalent to the PY approximation. Coupled with Eq. (1), Eq. (8) can be solved to yield $g(r)$ for $r \geq R$ and $c(r)$ for $r < R$. Verlet has applied this scheme for the LJ fluids near the triple point by performing the MD simulation with 864 particles [12]. Different models for the hypothetical closure relation have been proposed in Refs. [13–15], where the right-hand side of Eq. (8b) is replaced by a better approximation, i.e., the modified HNC and mean-spherical approximations.

The extrapolation scheme is indispensable in order to calculate the bridge function for low temperature states in which the PDF tends to be far away from its asymptotic behavior, i.e., $g(r) = 1$. The present system sizes of $N = 4000$ and $32\,000$ are so large that L is long enough to assume $B(r) = 0$ for $r \geq L/2$. Thus we first test the following closure relation [16] :

$$g(r) = \begin{cases} g_{\mathrm{MD}}(r) , & r < R \quad (9a) \\ \exp[-\beta u_c(r) + \gamma(r)] , & r \geq R , \quad (9b) \end{cases}$$

with the choice of $R = L/2$, the largest extrapolating distance. Here $u_c(r)$ is the truncated potential as in the case of the MD simulations:

$$u_c(r) = \begin{cases} u(r) - u(R_c) , & r < R_c \quad (10a) \\ 0 , & r \geq R_c . \quad (10b) \end{cases}$$

The bridge function $B_{\mathrm{MD}}(r)$ is determined for distances where $g_{\mathrm{MD}}(r) \neq 0$ by substituting the solution of the coupled equation given by Eqs. (1) and (9) into Eq. (2) as follows:

$$B_{\mathrm{MD}}(r) = \begin{cases} \beta u_c(r) + \ln[g_{\mathrm{MD}}(r)] - \gamma(r) , & r < R \quad (11a) \\ 0 , & r \geq R . \quad (11b) \end{cases}$$

To solve the integral equation, we have used an iterative procedure introduced by Ng [25]. The number of grid points and step size used in numerical integrations are 1024 points and $\Delta r = 0.025a$, respectively. Using $c(r)$ obtained by the HNC equation as an initial input function, it takes about 10 000 iterations to achieve

$$\left(\int |c_{\mathrm{in}}(r) - c_{\mathrm{out}}(r)|^2 r^2 dr\right)^{1/2} < 5 \times 10^{-9} , \qquad (12)$$

where $c_{\mathrm{in}}(r)$ and $c_{\mathrm{out}}(r)$ are the input and output functions, respectively. This ensures a consistency between the raw PDF data and solution of the integral equation given by Eqs. (1) and (2) with $u_c(r)$ and $B(r) = B_{\mathrm{MD}}(r)$. The computational time required for the iterative calculation is about 10 sec on a vector processor VP2600/10 computer with the vectorized fast-Fourier-transform routine.

Figures 2 and 3 show the bridge function obtained from the PDF data of the MD simulations for the LJ fluid and liquid aluminum. The reliability of $B(r)$ obtained from the 32 000-particle simulation can be confirmed in the case of the LJ fluid by the comparison with the result from the Monte Carlo simulation [26] calculating the cavity function as shown in Fig. 2. Although the oscillatory behavior of $B_{\mathrm{MD}}(r)$ is roughly independent of N and R_c, it is clearly seen for both model liquids that $B_{\mathrm{MD}}(r)$ calcu-

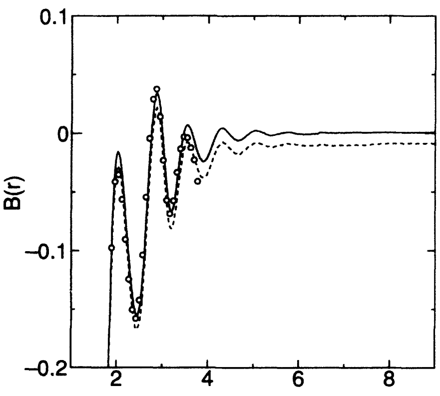

FIG. 2. The bridge function of the Lennard-Jones fluid obtained from the MD simulation using a longer extrapolating distance $R = L/2$. The full curve represents the result of $N = 32\,000$ and the dotted curve that of $N = 4000$, which has a spurious negative plateau due to the statistical noise. The result of the Monte Carlo simulation [26] is indicated by ○.

lated from data of $N = 4000$ yields a negative plateau for long-range distances, which vanishes smoothly at $r = R$. A similar plateau is also found in Ref. [15] where, instead of the HNC approximation, the mean-spherical approximation is used for extrapolating the simulation data. By varying the number of samples of the PDF, which is proportional to $N(N-1)$ and sampling steps, we have examined the behavior of this plateau. It is found that the plateau tends to zero when the number of samples increases even in the case of $N = 4000$ and the amplitude of the plateau is almost inversely proportional to the square root of the number of samples. Furthermore the difference of the raw PDF data for $N = 4000$ and $N = 32\,000$ is found to be extraordinarily larger than that expected by the finite-size effect discussed in Refs. [13,27]. Thus we have confirmed that the negative plateau of $B_{\mathrm{MD}}(r)$ comes from the statistical error of the raw PDF data, which can be reduced by increasing either N or the sampling steps.

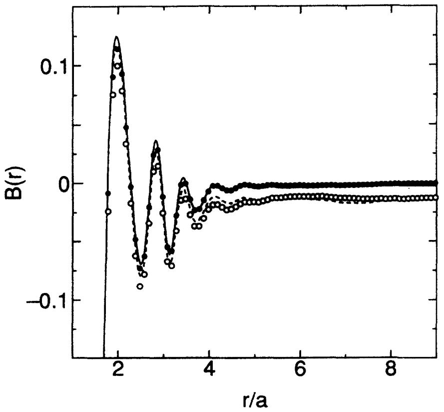

FIG. 3. The bridge function of liquid aluminum obtained from the MD simulation using a longer extrapolating distance $R = L/2$. Curves represent results for $R_c = 5.31a$: full curve, $N = 32\,000$; dotted curve, $N = 4000$. Symbols represent results for $R_c = 9.89a$: •, $N = 32\,000$; ○, $N = 4000$. The large-size simulation ($N = 32\,000$) indicates that the bridge function (full curve) for the truncated potential at $R_c = 5.31a$ is almost the same as that (•) for the larger cutoff $R_c = 9.89a$ and that the negative plateaus (○, dotted curve) are spurious due to the statistical noise.

As we have seen, the accurate $B(r)$ can be obtained by using a large system size with Eq. (9) and $R = L/2$. It is, however, useful for practical applications to find a procedure to extract a reliable $B(r)$ from the MD data of a small system size. Taking the results for $N = 32\,000$ as a reference data of the bridge function, we have examined the extrapolation method by taking R of 3 to 4 interatomic spacing, i.e., $R \simeq 5a$ to $7a$ in order to reduce the statistical-noise effect contained in $g_{\mathrm{MD}}(r)$. It is clearly seen from Figs. 4 and 5 that $B_{\mathrm{MD}}(r)$ for $N = 4000$ with a short extrapolating distance R fairly well agrees with the result for $N = 32\,000$ with $R = L/2$. From tests of the stability of $B_{\mathrm{MD}}(r)$ against the number of samples, about 10^{10} to 10^{11} samples of the PDF are found to be enough for the calculation of $B_{\mathrm{MD}}(r)$ by the present method of Eq. (9) and $R \simeq 5a$ to $7a$ without missing characteristics of the bridge function.

For the extrapolation scheme of Eq. (9), it is possible to use another type of approximate closure relations. For example, an extension of the raw PDF data by the mean spherical approximation is given by [14,15]

$$g(r) = g_{\mathrm{MD}}(r)\,, \qquad r < R \tag{13a}$$

$$c(r) = -\beta u(r)\,, \qquad r \geq R\,. \tag{13b}$$

In order to test the stability of the present extrapolation scheme against the choice of the extending closure relation, we have solved Eq. (13) coupled with Eq. (1) for both the LJ fluid and liquid aluminum with $R = R_c$ and found that Eq. (13) practically gives the same results as

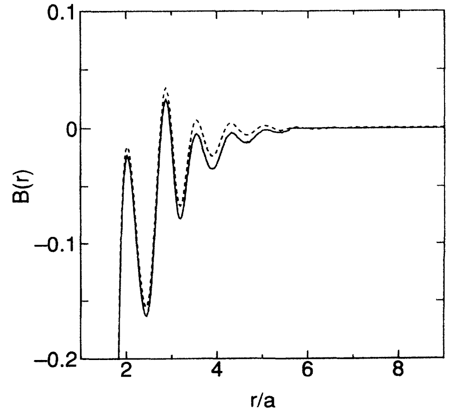

FIG. 4. The bridge functions of the Lennard-Jones fluid obtained from the MD simulation. The full curve represents the result of $N = 4000$ with $R = 3.7\sigma$ and the dotted curve that of $N = 32\,000$ with $R = L/2$.

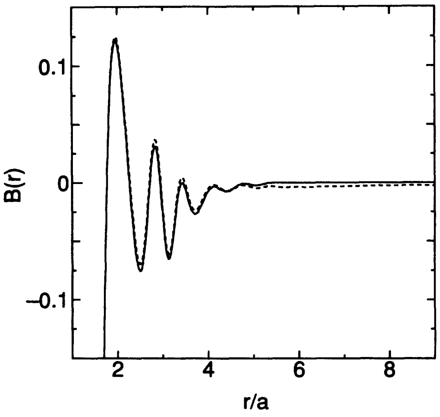

FIG. 5. The bridge function of liquid aluminum obtained from the MD simulation with the cutoff radius $R_c = 5.31a$. The full curve represents the result of $N = 4000$ with $R = R_c$ and the dotted curve that of $N = 32\,000$ with $R = L/2$. The spurious plateau caused by the statistical noise is deleted in the extracted $B(r)$ (full curve) of the small-size MD by taking a short extrapolating distance $R = 5.31a$, even when that (dotted curve) of the large-size MD still has a shallow plateau due to a large $R = L/2$.

Eq. (9). This is due to the fact that the direct correlation function smoothly approaches its asymptotic behavior of

$$c(r) \simeq -\beta u(r) \tag{14}$$

for $r \gtrsim 5a$, as seen from Fig. 6. For the LJ fluids, however, it is necessary to pay special care in choosing R in Eq. (13) because the direct correlation function deviates from its asymptotic behavior of Eq. (14) for $r \lesssim 6a$.

B. Comparison with approximate theories

For comparison between the present results for $B_{\mathrm{MD}}(r)$ and the bridge function of approximate theories, we have solved the integral equation for the LJ fluid and liquid aluminum with the reference HNC (RHNC) and variational modified HNC (VMHNC) approximations [3,4]. The approximate bridge function of the RHNC and VMHNC approximations are taken to be $B_{\mathrm{HS}}^{\mathrm{VW}}(r;\eta)$, the bridge function of the hard-sphere fluid with Verlet-Weis and Henderson-Grundke parametrizations [6], and $B_{\mathrm{HS}}^{\mathrm{PY}}(r)$ of Percus-Yevick equation [7], respectively, with η the packing fraction of the hard-sphere fluid. The optimal packing fraction is determined by

$$\frac{1}{2}\rho \int [g(r) - g_{\mathrm{HS}}^{\mathrm{VW}}(r;\eta)] \frac{\partial B_{\mathrm{HS}}^{\mathrm{VW}}(r;\eta)}{\partial \eta} d\mathbf{r} = 0 \tag{15}$$

for the RHNC equation [3] and

$$\frac{1}{2}\rho \int [g(r) - g_{\mathrm{HS}}^{\mathrm{PY}}(r;\eta)] \frac{\partial B_{\mathrm{HS}}^{\mathrm{PY}}(r;\eta)}{\partial \eta} d\mathbf{r} + \frac{\partial}{\partial \eta}[f_{\mathrm{PYV}}(\eta) - f_{\mathrm{CS}}(\eta)] = 0\,, \tag{16}$$

for the VMHNC equation [4]. Here $f_{\mathrm{PYV}}(\eta)$ is the reduced Helmholtz free energy of the reference hard-sphere fluid obtained from the virial equation with the Percus-Yevick approximation and $f_{\mathrm{CS}}(\eta)$ is that of Carnahan-Starling parametrization [28]. The optimal packing fraction obtained for the LJ fluid is $\eta = 0.4743$ and 0.4457 for the RHNC and VMHNC equations, respectively; for liquid aluminum, $\eta = 0.4513$ and 0.4234 for the RHNC and VMHNC equations, respectively.

Figures 7 and 8 show the bridge function of the RHNC and VMHNC approximations together with the results of the MD simulation. It is easily seen that the core region ($r \lesssim 2a$) of $B_{\mathrm{MD}}(r)$ is well reproduced for both liquids by both approximations, which supports a universal behavior of the short-range part of the bridge function pointed out by Rosenfeld and Ashcroft [2]. This is, however, not the case for the intermediate range of $B(r)$. For both model liquids, the bridge function of the RHNC and VMHNC approximations yields a clear discrepancy from

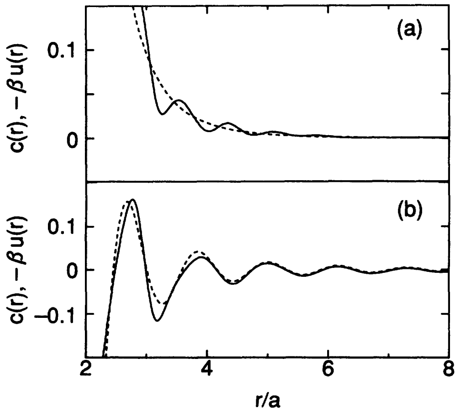

FIG. 6. Asymptotic behavior of the direct correlation function $c(r)$ obtained from the MD simulation: (a) result for the LJ fluid with $N = 32\,000$ and $R = L/2$; (b) result for liquid aluminum with $R_c = 9.89a$, $N = 32\,000$, and $R = L/2$. The full curve represents $c(r)$ and the dotted curve $-\beta u(r)$. Note that the asymptotic behavior is different between the LJ fluid and liquid aluminum.

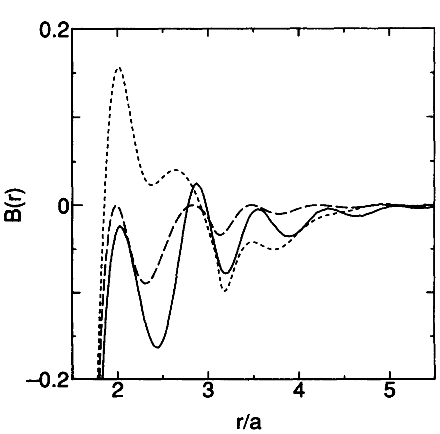

FIG. 7. Comparison of the bridge functions for the LJ fluid obtained from the MD simulation with $N = 4000$ and $R = 3.7\sigma$ (full curve), the RHNC approximation (dotted curve), and the VMHNC approximation (dashed curve).

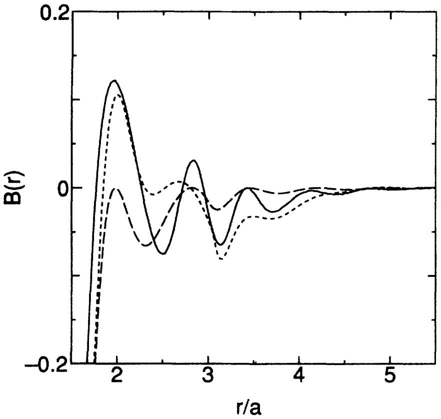

FIG. 8. Comparison of the bridge functions for liquid aluminum obtained from the MD simulation with $N = 4000$ and $R = R_c = 5.31a$ (full curve), the RHNC approximation (dotted curve), and the VMHNC approximation (dashed curve).

the result of the MD simulation; the structures of the RHNC and VMHNC bridge functions are the same for both the LJ fluid and liquid aluminum irrespective of the different character of their potentials, while the MD bridge function exhibits a dependence on the potential. This discrepancy in the bridge function between the MD simulation and approximate theories practically gives no serious effects on the first peak of the PDF and thermodynamic quantities such as the internal energy. But details of the PDF for $2a \lesssim r \lesssim 5a$ are actually different between approximate theories and the MD simulation in a similar way, as discussed in Ref. [9]. Such a difference is essentially caused by the distinctive oscillatory behavior of the bridge function at intermediate-range distances as seen from Figs. 7 and 8, which considerably depends on details of the pair potential.

IV. CORRECTION TO THE PAIR DISTRIBUTION FUNCTION

The effective pair potential between ions in liquid metals shows a marked difference from the LJ potential: liquid metals have a soft repulsive core and long-range oscillatory tail. Because the computer simulation requires a truncation of the pair potential, it is particularly interesting to investigate whether this truncation affects the behavior of the PDF obtained by the simulation. If the raw PDF data of the MD simulation has a dependency on the truncation of the potential, $B_{\mathrm{MD}}(r)$ together with the Ornstein-Zernike relation can be used for correcting the raw PDF data because the bridge function extracted from the MD simulation is insensitive to the choice of the cutoff radius, as we have seen in Sec. III.

For both the LJ fluid and liquid aluminum, we have tested the following closure relation in order to obtain the PDF for the full potential $u(r)$:

$$g(r) = \begin{cases} \exp[-\beta u(r) + \gamma(r) + B_{\mathrm{MD}}(r)]\,, & \\ \quad g_{\mathrm{MD}}(r) \neq 0 & \text{(17a)} \\ 0\,, \;\; g_{\mathrm{MD}}(r) = 0. & \text{(17b)} \end{cases}$$

Note that Eq. (17) is different from Eq. (9) in that the potential is an uncut one. Figure 9 shows the raw PDF data of the MD simulation for liquid aluminum with two different cutoff radii ($R_c = 5.31a$ and $9.89a$) together with the result of Eq. (17) using $B_{\mathrm{MD}}(r)$ obtained in the case of $N = 4000$ and $R_c = 5.31a$. It is clearly seen that these two raw PDF data show a remarkable difference for $r \gtrsim 4a$, which proves a strong effect of the long-range oscillatory tail of the effective ion-ion potential for liquid aluminum. A similar result has also been reported by Matsuda *et al.* for liquid cesium with the modified HNC integral equation [11]. As seen from Fig. 9, the solution of Eq. (17) and the Ornstein-Zernike relation gives an excellent result which reproduces the raw PDF data of the large-size MD with $R_c = 9.89a$ up to $r \simeq 8a$ even if $B_{\mathrm{MD}}(r)$ of the small-size MD with $R_c = 5.31a$ is applied. In Fig. 9 the discrepancy between the solution of Eq. (17) and the raw PDF data for $R_c = 9.89a$ is apparent for $r \gtrsim 8a$: this discrepancy is interpreted as an artifact due to the truncated potential for the raw PDF data because the integral equation with $B_{\mathrm{MD}}(r)$ for $R_c = 5.31a$ and $9.89a$ gives the same result within numerical accuracy. In the case of the LJ fluid, however, we cannot find any differences in the PDF between the raw simulation data and results obtained by Eq. (17). This is understood as a result of the short-range nature of the LJ potential, and the truncation error in the PDF does not appear in the simulation with use of this cut potential. Note that, despite a marked difference in the bridge function between approximate theories and the MD simulation, the PDF's obtained by the RHNC and VMHNC equations agree well with the result of the integral equation with the extracted bridge function for $r \gtrsim 5a$, in contrast to the result of Lomba *et al.* [15], where a significant difference is found between them in that region.

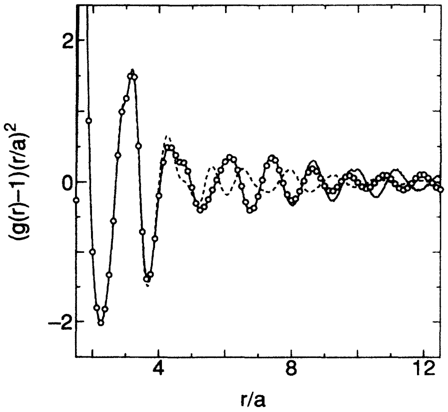

FIG. 9. Comparison of the raw PDF data for liquid aluminum obtained from the MD simulation with $N = 32\,000$: dotted curve, $R_c = 5.31a$; full curve, $R_c = 9.89a$. The raw PDF (full curve) for $R_c = 9.89a$ shows good agreement up to near its cutoff distance $R_c = 9.89a$ with the solution (○) of the integral equation with the extracted bridge function from the small-size MD ($N = 4000$) for the truncated potential at $R_c = 5.31a$. The PDF of the integral equation with the extracted bridge function becomes identical to those of the RHNC and VMHNC equations for $r \gtrsim 5a$.

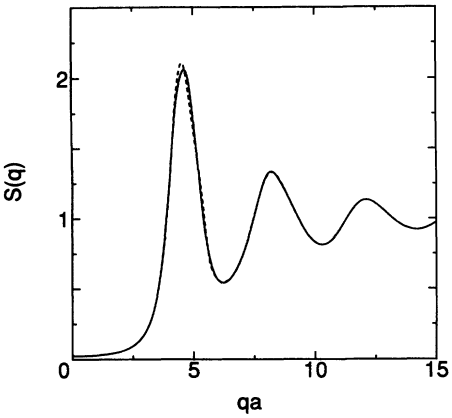

FIG. 10. Comparison of the static structure factors for liquid aluminum obtained from the MD simulation with $N = 4000$ and $R_c = 5.31a$: the full curve is from Eq. (9); the dotted curve is from Eq. (17). The structure factor (full curve) of the truncated potential shows a distinguishable difference from that (dotted curve) of the uncut potential.

Improvement of the raw simulation data with Eq. (17) is also able to apply for calculations of the static structure factor $S(q)$ defined by

$$S(q) = 1 + \rho \int \exp[-i\mathbf{q} \cdot \mathbf{r}][g(r) - 1]d\mathbf{r} \,. \qquad (18)$$

Figure 10 shows two static structure factors for liquid aluminum: one for the truncated potential calculated from the extended PDF data with Eq. (9) and the other for the full potential obtained from Eq. (17). It is clearly seen that characteristics of the first peak of $S(q)$ are largely altered by the truncation of the pair potential: the peak height for the truncated potential is smaller than that for the full potential and the peak position for the full potential is shifted toward the origin.

V. DISCUSSION

We have performed extensive MD simulations for the dense LJ fluid and liquid aluminum with 4000 and 32 000 particles. The bridge function, whose properties are important for a practical application of the integral equation theory, has been extracted from the PDF data of the MD simulation by using the HNC approximation for extrapolating the raw PDF data. The extracted bridge function in this way is found to be sensitive to the statistical noise in the raw PDF data, yielding a spurious negative plateau at long-range distances, when the extrapolating distance is chosen to be half of the side length of the simulation cell. It is important to take the extrapolating distance as short as $5a$ to $7a$ with a discarding of the PDF data outside that distance; then, the effect of statistical noise contained in the raw simulation data is successfully reduced and the present procedure provides a good result for the bridge function even in the case of relatively inaccurate data of $N = 4000$. The extracted bridge function is found to depend less on the system size and the cutoff radius used in the simulation. The extension of the simulation data by the mean spherical approximation gives the same results as the present procedure because the asymptotic behavior of the direct correlation function is attained for $r \gtrsim 5a$ for both model liquids.

The short-range part of the bridge function obtained from the MD simulation is well reproduced by the RHNC and VMHNC approximations, supporting a universality of the short-range part of the bridge function pointed out by Rosenfeld and Ashcroft [2]. The intermediate-range part of the bridge function, however, is found to depend on details of the pair potential used in the simulation, resulting in a discrepancy in the intermediate-range part of the PDF's obtained by the computer simulation and approximate integral equation.

For liquid aluminum whose effective ion-ion potential is accompanied by the long-range oscillatory tail, the MD simulations with different cutoff radii yield different behaviors of the long-range part of the PDF. In order to correct the error of the raw PDF data due to the truncation in the potential, we have evaluated the integral equation for the uncut potential coupled with the extracted bridge function from the MD simulation, utilizing the insensibility of the bridge function to the cutoff radius of the potential used in the MD simulation. It is found that the integral equation with the extracted bridge function successfully improves the long-range part of the PDF, which agrees well with the raw PDF data with a large cutoff radius. The improving method of the raw simulation data is also applied to get the static structure factor, providing a higher first peak than that obtained by the extrapolation procedure with the truncated potential. The present result suggests that the comparison of the raw simulation data with experimental data as well as results of approximate theories requires special care, especially for some liquid metals. At least it is possible for the significant truncation error in the PDF to appear for liquid metals interacting via such a potential with a positive minimum as the model potential for aluminum.

The present extrapolation procedure can be applied for various model liquids, including binary mixtures, and provides their accurate bridge functions at the same time. The resultant bridge function can be used further for improving approximate theories for the integral equation by taking it as a reference datum, and also for applying it to the quantal HNC theory [29] in constructing effective pair potentials of liquid metal by utilizing the MD correlation functions for the uncut potential. Finally, calculations of the bridge function for liquid alkali metals by the present procedure are now undertaken for testing the applicability of the extrapolation scheme for different liquid metals.

ACKNOWLEDGMENTS

We would like to thank Computing and Information Systems Center of Japan Atomic Energy Research Institute (JAERI) for permitting us an exhausting use of the dedicated vector-parallel processor Monte-4 computer. One of us (S. K.) would like to thank Mr. K. Higuchi (JAERI) for useful hints on the effective sampling of the PDF in the MD simulation.

[1] J. P. Hansen and I. R. McDonald, *Theory of Simple Liquids*, 2nd ed. (Academic, London, 1986).
[2] Y. Rosenfeld and N. W. Ashcroft, Phys. Rev. A **20**, 1208 (1979).
[3] F. Lado, Phys. Lett. **89**, 196 (1982); F. Lado, S. M. Foiles, and N. W. Ashcroft, Phys. Rev. A **28**, 2374 (1983).
[4] Y. Rosenfeld, Phys. Rev. A **29**, 2877 (1984).
[5] S. M. Foiles, N. W. Ashcroft, and L. Reatto, J. Chem. Phys. **80**, 4441 (1984).
[6] L. Verlet and J. J. Weis, Phys. Rev. **45**, 939 (1972); D. Henderson and E. W. Grundke, J. Chem. Phys. **69**, 601 (1975).
[7] M. S. Smith and D. Henderson, Mol. Phys. **19**, 411 (1970).
[8] S. Labík and A. Maijevský, Mol. Phys. **67**, 431 (1989).
[9] S. Kambayashi and Y. Hiwatari, Phys. Rev. A **41**, 1990 (1990).
[10] D. Gazzillo and R. G. Della Valle, J. Chem. Phys. **99**, 6915 (1993).
[11] N. Matsuda, K. Hoshino, and M. Watabe, J. Chem. Phys. **93**, 7350 (1990).
[12] L. Verlet, Phys. Rev. **165**, 201 (1968).
[13] S. M. Foiles, N. W. Ashcroft, and L. Reatto, J. Chem. Phys. **81**, 6140 (1984).
[14] P. D. Poll and N. W. Ashcroft, in *Proceedings of the NATO Advanced Research Workshop on Strongly Coupled Plasma Physics, Santa Cruz, 1986*, edited by F. J. Rogers and H. E. DeWitt (Plenum, New York, 1987), p. 35.
[15] E. Lomba, M. Alvarez, G. Stell, and J. A. Anta, J. Chem. Phys. **97**, 4349 (1992).
[16] S. Kambayashi and Y. Hiwatari, J. Non-Cryst. Solid **156-158**, 80 (1993).
[17] N. W. Ashcroft, Phys. Lett. **23**, 48 (1966).
[18] R. Taylor, J. Phys. F **48**, 1699 (1978).
[19] D. J. W. Geldart and R. Taylor, Can. J. Phys. **48**, 167 (1970).
[20] M. L. Cohen and V. Heine, *Solid State Physics* (Academic, New York, 1970), Vol. 33, p. 1.
[21] W. G. Hoover, A. J. C. Ladd, and B. Moran, Phys. Rev. Lett. **48**, 1818 (1982); W. G. Hoover, *Molecular Dynamics* (Springer, Berlin, 1986).
[22] B. Bernu, Physica **122A**, 129 (1983).
[23] S. Kambayashi and Y. Hiwatari, Phys. Rev. E **49**, 1251 (1994).
[24] K. Asai, K. Higuchi, M. Akimoto, H. Matsumoto, and Y. Seo, in *Proceedings of the Joint International Conference on Mathematical Methods and Supercomputing in Nuclear Applications, Karlsruhe, 1993*, edited by H. Künster, E. Stein, and W. Werner (Kernforschungszentrum, Karlsruhe, 1993), p. 341.
[25] K. C. Ng, J. Chem. Phys. **61**, 2680 (1974).
[26] M. Llano-Restrepo and W. G. Chapman, J. Chem. Phys. **97**, 2046 (1992).
[27] J. L. Lebowitz and J. K. Percus, Phys. Rev. **122**, 1675 (1961).
[28] N. F. Carnahan and K. E. Starling, J. Chem. Phys. **51**, 635 (1969).
[29] J. Chihara, Phys. Rev. A **33**, 2575 (1986).